Model of Peptide Bond−Aromatic Ring Interaction: Correlated Ab Initio Quantum Chemical Study

Lada Bendová,[†] Petr Jurečka,[‡] Pavel Hobza,*[,†,‡] and Jiří Vondrášek*[,†]

Institute of Organic Chemistry and Biochemistry, Academy of Sciences of the Czech Republic, and Center for Biomolecules and Complex Molecular Systems, Flemingovo namesti 2, 166 10 Prague 6, Czech Republic, and Department of Physical Chemistry and Center for Biomolecules and Complex Molecular Systems, Palacký University, Tr. Svobody 26, 771 46 Olomouc, Czech Republic

Received: April 12, 2007; In Final Form: June 14, 2007

Aromatic ring−peptide bond interactions (modeled as benzene and formamide, *N*-methylformamide and *N*-methylacetamide) are studied by means of advanced computational chemistry methods: second-order Möller−Plesset (MP2), coupled-cluster single and double excitation model [CCSD(T)], and density functional theory with dispersion (DFT-D). The geometrical preferences of these interactions as well as their interaction energy content, in both parallel and T-shaped arrangements, are investigated. The stabilization energy reaches a value of over 5 kcal/mol for the *N*-methylformamide−benzene complex at the CCSD(T)/complete basis set (CBS) level. Decomposition of interaction energy by the DFT-symmetry-adapted perturbation treatment (SAPT) technique shows that the parallel and T-shaped arrangements, although similar in their total interaction energies, differ significantly in the proportion of electrostatic and dispersion terms.

Introduction

The stability of protein tertiary structure is a result of an interplay between various noncovalent interactions, which contribute to the overall stability of the protein molecule because of their frequent occurrence. Besides the long-recognized forces, for example, H-bonds and salt bridges, there are abundant van der Waals interactions, among which the aromatic interactions such as $\pi-\pi$ stacking and XH$-\pi$ H-bonding have been shown to also play an important role for protein structure,[1] as well as protein−ligand recognition.[2]

The first to point out the importance of aromatic interactions in proteins were Burley and Petsko[3] in a work on interaction between phenylalanine residues. The strength of the stabilization energy in Phe pairs was estimated to be 1−2 kcal/mol[4−6] by gas-phase calculations of benzene and toluene dimer model systems. In the benzene dimer model, two minima exist—parallel displaced arrangement and T-shaped arrangement—both stabilized by favorable dispersion and quadrupole−quadrupole electrostatic interaction.[7,8]

It is worth mentioning that $\pi-\pi$ stacking is not strictly defined as an interaction of aromatic systems; it is a more general phenomenon that includes interactions of planar systems with delocalized orbitals, such as peptide bonds. Analogically, the XH$-\pi$ bonding is not limited to aromatic−aromatic interaction, because the aromatic ring can serve as an acceptor for nonaromatic H-bond donors.[9] It has been shown by gas-phase calculations[10] that both electrostatic and dispersion terms are important in the XH$-\pi$ interaction. The directionality of the interaction is mainly controlled by the electrostatic term; however, the potential energy surface is very flat near the minimum due to the long-range dispersion term.

In proteins, the interactions of an aromatic ring with a nonaromatic moiety have been subject of an exhaustive Protein Data Bank (PDB) mining study,[11] which revealed a relatively high occurrence of such interactions (1 per 10.8 aromatic amino acids). A large fraction of these interactions are NH$-\pi$ contacts. This finding can be attributed to the abundance of potential NH donors in the protein backbone as well as in the side chains of some residues. Moreover, the size of the aromatic ring together with the broad minimum of the potential energy surface makes it a good substitute in the case where conventional H-bond acceptors are locally absent. Therefore the aromatic−amide interaction is one of the most common weak interactions in proteins. Several studies[4,12,13] have shown that the N bearing groups prefer to lie above the aromatic ring. However, only a fraction of these contacts can be considered to be H-bonds; the NH$-\pi$ interactions are in fact outnumbered by the aromatic−amide stacked structures[12,14] with the sp^2-hybridized N atom. This finding is in accordance with the higher number of conventional H bonds the NH group can form in the stacked orientation.[15] The significance of the aromatic−amide interaction for stabilization of secondary structure and local motifs has been proved by PDB mining.[16] It includes stabilization of α-helix termini and β-sheet edges as well as regular turns.[11] The aromatic ring−peptide bond interaction has also been shown to be important in certain biological recognition processes.[17]

The aromatic−amide interaction has previously been studied with a benzene−formamide model.[18] The authors performed a restricted optimization and reported counterpoise-corrected interaction energy values of 4.0 and 2.0 kcal/mol for the T-shaped and the stacked complex, respectively, at the MP2/6-311G(2d,2p) gas-phase level. Another study explored the T-shaped arrangement of the *N*-methylformamide (NMF)−benzene complex[19] at the MP2/6-31G** level with counterpoise correction. The maximum gas-phase stabilization energy found

* Corresponding authors: fax (+420) 220-410-320; e-mails: jiri.vondrasek@uochb.cas.cz, pavel.hobza@uochb.cas.cz.

[†] Institute of Organic Chemistry and Biochemistry, Academy of Sciences of the Czech Republic, and Center for Biomolecules and Complex Molecular Systems.

[‡] Department of Physical Chemistry and Center for Biomolecules and Complex Molecular Systems, Palacký University.

10.1021/jp072859+ CCC: $37.00
Published on Web 08/02/2007

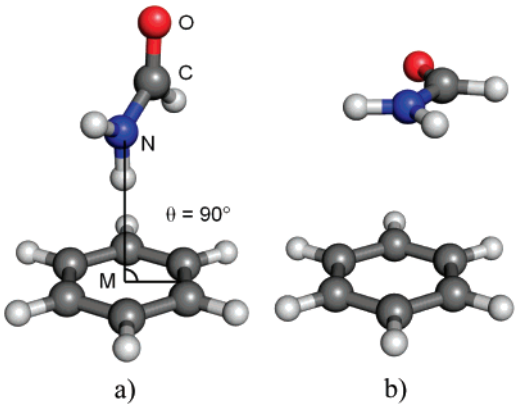

Figure 1. Initial geometries of FMA−benzene complex: (a) T-shaped arrangement and (b) stacked arrangement. M, center of benzene ring; θ, angle between the plane of benzene ring and the NCO plane of the peptide bond moiety.

was 4.4 kcal/mol. In our previous study[20] we examined the interaction between a phenylalanine residue and a peptide bond (modeled as *N*-methylformamide) in the crystal structure of the small protein rubredoxin with high-level ab initio calculations. The interaction energy determined by use of coupled-cluster single and double excitation model [CCSD(T)] at the complete basis set limit (CBS) amounted to −8.2 kcal/mol. Such an unexpectedly strong interaction motivated us to investigate the aromatic−amide interaction in more detail. Another reason is that the above-mentioned studies employed a standard computational level, which might have affected the quality of the results.

In this work we investigate spatial preferences of aromatic ring−peptide bond interaction. We aim at investigating complexes representative of the arrangements found in protein structure. We optimize geometries and calculate interaction energies for both parallel and T-shaped arrangements. Further, we uncover the underlying forces governing the directional preferences of the interaction using interaction energy decomposition.

Computational Methods

RI-MP2 Gradient Optimization. We use the RI-MP2/cc-pVTZ method for optimization of all subsystems [benzene, formamide (FMA), *N*-methylformamide (NMF), and *N*-methylacetamide (NMA)] as well as a reference method for optimization of the complexes. The resolution of identity (RI) procedure is used to make the calculations more economic.

CCSD(T)/CBS Interaction Energy. In the optimized complexes, the CCSD(T)/CBS interaction energy is approximated as

$$\Delta E_{\mathrm{CCSD(T)}}{}^{\mathrm{CBS}} = \Delta E_{\mathrm{MP2}}{}^{\mathrm{CBS}} + (\Delta E_{\mathrm{CCSD(T)}} - \Delta E_{\mathrm{MP2}})^{\text{small basis set}} \quad (1)$$

The former term is determined by use of the two-point Helgaker extrapolation scheme.[21] The Hartree−Fock and correlation MP2 energies necessary for the extrapolation are determined at the RI-MP2/aug-cc-pVXZ (X = D, T) level. The CCSD(T) term is calculated with a smaller basis set, 6-31G*(0.25) (the exponent of d-functions changed from standard value of 0.8 to a more diffuse one of 0.25). The difference between the MP2 and CCSD(T) interaction energies does not strongly depend on basis set size (unlike the interaction energies themselves); thus the 6-31G*(0.25) basis set already gives satisfactory values for this difference.[22] The deformation energy E^{def} is determined as the difference between the energy of isolated subsystems in the complex geometry and the energy of the supersystem is also calculated at the RI-MP2/cc-pVTZ level to correct the interaction energy. The total interaction energy is calculated as

CHART 1: Systems Studied in Interaction with Benzene

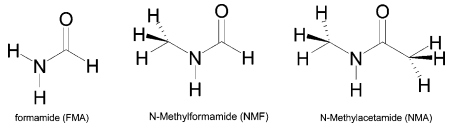

$$\Delta E^{\mathrm{total}} = \Delta E_{\mathrm{CCSD(T)}}{}^{\mathrm{CBS}} + \Delta E^{\mathrm{def}}$$

All interaction energies are counterpoise-corrected for basis-set superposition error (BSSE).

Interaction Energy by Use of DFT Functionals. Both the B3LYP functional,[23] which is commonly used for calculating biopolymers, and the PWB6K functional designed by Zhao and Truhlar[24] are tested for their ability to correctly describe the interaction in the studied complexes. These two functionals are used with the 6-31G** basis set on the geometries obtained by MP2/cc-pVTZ optimization.

RI-DFT-D Optimization. The RI-DFT-D (DFT with an empirical dispersion term[25]) optimization is performed with the TPSS functional and extended Pople-type basis set [6-311++G-(3df,2pd), denoted as LP]. The interaction energy of the optimized complexes is calculated at the same level. The BSSE at this level is negligible due to the large basis set employed, and it is thus not necessary to correct the interaction energy for its effect.

Symmetry-Adapted Perturbation Treatment. Components of the total interaction energies are determined by DFT-symmetry-adapted perturbation treatment (SAPT).[26,27] Calculations are performed for T-shaped and tilted T-shaped structures of the NMA−benzene complex optimized by RI-MP2/cc-pVTZ as well as for a set of stacked structures varying in the NM distance. PBE0AC exchange−correlation functional with density fitting and the aug-cc-pVDZ basis set are used. The aug-cc-pVDZ set is large enough to provide a reliable estimate of the electrostatic, induction, and exchange components (note that the SAPT calculations are not burdened with the BSSE). Although this basis set underestimates the dispersion component by about 10−20%,[27] it should nevertheless serve well for the purpose of comparing relative strengths of this term in different arrangements.

In SAPT, total interaction energy E_{int} is calculated as a sum of electrostatic, exchange, induction, and dispersion components, with the dispersion and induction components also having their exchange counterparts:

$$E_{\mathrm{int}} = E^1{}_{\mathrm{pol}} + E^1{}_{\mathrm{ex}} + E^2{}_{\mathrm{ind}} + E^2{}_{\mathrm{ex-ind}} + E^2{}_{\mathrm{disp}} + E^2{}_{\mathrm{ex-disp}} + \delta\mathrm{HF} \quad (2)$$

The exponents in eq 2 refer to the intermolecular perturbation order. E^1 is defined as the sum of $E^1{}_{\mathrm{pol}}$ and $E^1{}_{\mathrm{ex}}$, and E^2 is the sum of $E^2{}_{\mathrm{ind}}$, $E^2{}_{\mathrm{ex-ind}}$, $E^2{}_{\mathrm{disp}}$, and $E^2{}_{\mathrm{ex-disp}}$ energies, respectively. δHF denotes the estimate for higher-order contributions. In the present study, we do not use the standard SAPT method (which is prohibitively expensive for the complexes investigated) but employ its DFT version,[26,27] in which the intramolecular correlation is treated fully by the DFT, whereas the intermolecular interaction is calculated by perturbational treatment. Since perturbation theory exploits orbital energies, the inherently

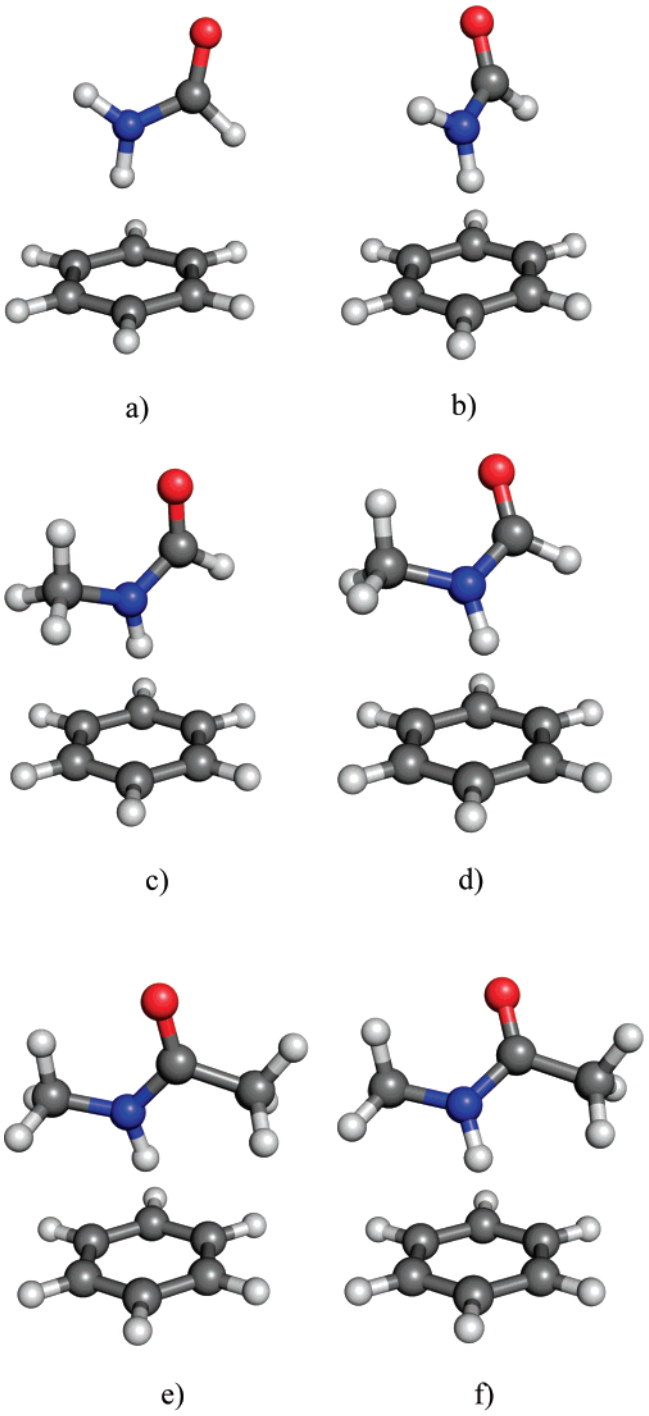

Figure 2. Geometries of optimized complexes: (a) FMA−benzene starting from T-shaped arrangement; (b) FMA−benzene starting from stacked arrangement; (c) NMF−benzene starting from T-shaped arrangement; (d) NMF−benzene starting from stacked arrangement; (e) NMA−benzene starting from T-shaped arrangement; (f) NMA−benzene starting from stacked arrangement.

incorrect DFT orbitals are corrected by gradient-controlled shift procedure,[26,27] with the difference (shift) between the vertical ionization potential (IP) and highest occupied molecular orbital (HOMO) energy of the DFT method employed as an input. Herein the IPs are calculated at the PBE0/TZVP level while the HOMO values are taken from the aug-cc-pVDZ calculation. Our shift values are 0.0715 and 0.0855 Eh for benzene and NMA, respectively.

We use Gaussian 03,[28] Turbomole,[29] and MOLPRO[30] codes as well as our own code for RI-DFT-D calculations.[25]

TABLE 1: Geometrical Parameters of Optimized X−Benzene Complexes[a]

	MP2/cc-pVTZ		RI-DFT-D	
system	NM,[b] Å	θ,[c] deg	NM,[b] Å	θ,[c] deg
NMA_T	3.221	89	3.569	88
NMA_S	3.188	52	3.422	58
NMF_T	3.210	74	3.420	83
NMF_S	3.144	55	3.374	56
FMA_T	3.274	83	3.524	86
FMA_S	3.259	68	3.342	31

[a] X = NMA, NMF, and FMA. [b] Distance between the amide nitrogen of X and the benzene ring center (M). [c] Interplanar angle.

Results and Discussion

We use three models for the peptide bond moiety: formamide (FMA), *N*-methylformamide (NMF), and *N*-methylacetamide (NMA) (see Chart 1). Two main geometrical arrangements are possible for aromatic ring−peptide bond interactions: parallel and T-shaped, shown in Figure 1 for FMA and benzene. For the T-shaped arrangement, the angle between the plane of the benzene ring and the NCO plane of the peptide bond moiety $\theta = 90°$ (the planes are perpendicular) and the NH bond is directed toward the center of the benzene ring. For the parallel arrangement, the angle $\theta = 0°$ (the planes are mutually parallel) and the N atom lies in the C6 axis of benzene. We use the annotation _T and _S for T-shaped and stacked **starting** geometries, respectively.

Geometries of optimized complexes are shown in Figure 2, and the results of the geometry optimization are summarized in Table 1. The interacting complexes are characterized by the NM distance between the amide nitrogen N and the center of the benzene ring M. In geometry optimizations starting from the T-shape arrangement we observe only moderate differences between initial and final geometries in all three models. On the other hand, when starting from the parallel arrangement, the geometries undergo profound changes. The θ angle changes from the initial value of 0 degrees to values of about 50−70 degrees. (Hereafter, we term the structures characterized by θ angle values in the range of 20−70 degrees as tilted-T-shaped ones, discerning them from both strictly parallel with θ angle 0−20 degrees and strictly T-shaped with θ angle of 70−90 degrees.) The changes are similar for NMA and NMF complexes while being less profound for FMA. Although all three model systems pass from parallel arrangements to tilted-T-shaped ones, methylation evidently disfavors T-shape arrangement and favors the tilted-T-shape. Given the shallowness of the PES, the RI-DFT−D and MP2/cc-pVTZ results agree reasonably well, although the distances are slightly larger for DFT−D optimized complexes.

Table 2 shows energy characteristics for the optimized complexes. Columns 2−4 show MP2 interaction energies determined with the aug-cc-pVDZ and aug-cc-pVTZ basis sets and at the CBS limit, respectively. Passing to a larger basis set yields a substantial stabilization energy increase (~0.6 kcal/mol), and extrapolation to CBS limit yields even larger stabilization energies (the highest being 6.4 kcal/mol for NMA−benzene). However, it is known[22] that the MP2/CBS stabilization energies are overestimated and that the CCSD(T) correction term should be included. This term is positive, that is, of a repulsive character for all systems, being similar for both structures of NMA and NMF (~1 kcal/mol) and slightly smaller for both structures of FMA (~0.6 kcal/mol).

The final stabilization energies, E^{total}, including the deformation energy, are shown in column 8. Evidently, these energies

TABLE 2: Interaction Energies[a] for MP2/cc-pVTZ and RI-DFT−D Optimized Structures

system	aDZ	aTZ	CBS	ΔCCSD(T)	CCSD(T)/CBS	E^{def}	E^{total}	PWB6K	B3LYP	RI-DFT-D
NMA_T	−5.3	−6.0	−6.3	1.0	−5.3	0.3	−5.0	−4.2	0.4	−5.1
NMA_S	−5.4	−6.1	−6.4	1.1	−5.3	0.1	−5.2	−4.1	0.8	−5.3
NMF_T	−4.9	−5.6	−5.8	0.9	−5.0	0.0	−5.0	−4.2	−0.4	−5.0
NMF_S	−5.0	−5.7	−6.0	0.9	−5.1	0.1	−5.0	−4.2	0.0	−5.0
FMA_T	−4.3	−4.9	−5.2	0.6	−4.6	0.0	−4.6	−4.4	−1.0	−4.4
FMA_S	−4.3	−4.9	−5.2	0.6	−4.6	0.0	−4.6	−4.3	−0.9	−4.6

[a] Interaction energies are given in kilocalories per mole and were determined at various theoretical levels. aDZ, aTZ, and CBS denote aug-cc-pVDZ, aug-cc-pVTZ, and complete basis set limit, respectively. E^{def} is the deformation energy.

TABLE 3: Components of Interaction Energy for Structures of NMA−Benzene Complex[a]

	R (Å)	E^1_{pol}	E^1_{ex}	E^{2*}_{ind}[b]	E^{2*}_{disp}[c]	δHF	E^1	E^2	E_{int}	E^{2*}_{disp}/E^1_{pol}
T	3.2	−7.3	13.4	−1.8	−10.6	−1.3	6.1	−12.4	−7.1	1.45
tT	3.2	−8.0	15.3	−1.9	−11.6	−1.5	7.3	−13.5	−7.0	1.45
S	3.2	−9.3	24.9	−0.9	−15.3	−1.9	15.7	−16.3	−2.5	1.65
S	3.4[d]	−4.5	11.0	−0.6	−10.6	−0.8	6.5	−11.2	−5.5	2.36
S	3.5[d]	−3.4	8.1	−0.5	−9.2	−0.6	4.7	−9.7	−5.6	2.71
S	3.6[d]	−2.6	6.0	−0.5	−8.0	−0.4	3.4	−8.4	−5.5	3.08

[a] Components of interaction energy (T, T-shaped; tT, tilted T-shaped; S, stacked) are given in kilocalories per mole and were determined by DFT-SAPT. [b] $E^{2*}_{ind} = E^2_{ind} + E^{2*}_{ex-ind}$. [c] $E^{2*}_{disp} = E^2_{disp} + E^{2*}_{ex-disp}$. [d] Hydrogens of methyl group(s) optimized.

are similar to those obtained at the MP2/aug-cc-pVDZ level. This is due to a partial compensation of the stabilization energy increase between the aug-cc-pVDZ and the CBS level and the decrease brought by the CCSD(T) correction term. However, this compensation cannot be relied upon, as for some complexes the MP2/aug-cc-pVDZ method may yield substantially incorrect stabilization energies. We may conclude that the total stabilization energies are relatively high, varying from 4.6 kcal/mol for FMA−benzene to 5.2 kcal/mol for NMA−benzene. The magnitude of these interactions is comparable to classical H-bonding.

Columns 9 and 10 in Table 2 show DFT interaction energies determined with the recently introduced PWB6K functional and with the widely used B3LYP functional, respectively. The limited performance of the DFT procedure for stacked complexes caused by a lack of London dispersion energy in DFT methods is well-known. Evidently, the B3LYP functional completely fails and stabilization energies are strongly underestimated. The performance of the PWB6K functional is more promising. However, the PWB6K stabilization energies are systematically underestimated and do not reflect the effect of system size. The last column of Table 2 shows the RI-DFT-D stabilization energies for structures optimized at the same level. These results are very similar to the CCSD(T)/CBS ones; the effect of methylation is described correctly. This is in accord with the fact that the RI-DFT-D method is parametrized toward CCSD(T)/CBS values and therefore it is supposed to yield very accurate energies as well as geometries.[25] An interesting fact is that, for all models, the final interaction energies for T-shaped and tilted T-shaped arrangements do not differ too much. This suggests that the interaction hypersurface of these two systems is quite shallow and that no significant barrier exists between different local minima.

To elucidate the nature of these interactions in more detail, we determined the energy components using the perturbation DFT-SAPT technique. Table 3 shows the interaction energy components for NMA−benzene complexes in different arrangements. The interaction energies of T-shaped and tilted T-shaped structures are very similar and their components differ only moderately. The electrostatic energy (E^1_{pol}) is more attractive for the tilted T-shaped arrangement, but this growth is compensated by an increase of the exchange-repulsion term. The effective induction energy (E^{2*}_{ind}) is small for both arrangements. The effective dispersion term (E^{2*}_{disp}), which constitutes a major contribution to the overall stabilization, is larger for the tilted T-shaped structure, but again the difference is not significant.

Although no stacked arrangement minimum has been found by geometry optimizations, this arrangement is found in protein structures.[11] Therefore it would be interesting to see whether the described trends remain valid for this arrangement. Upon changing from the T-shaped to a parallel arrangement while the NM distance is kept constant, the interaction energy becomes much smaller (−2.5 vs −7.1 kcal/ mol). This is due to the enhanced repulsion between the methyl group(s) and benzene, reflected by a large exchange-repulsion term. To reduce this repulsion we optimize the position of methyl hydrogens and perform a scan along the NM axis. Table 3 shows that the optimal distance in the stacked arrangement is larger, with a value of 3.5 Å. The electrostatic energy is considerably less attractive in the parallel arrangement than in both the T-shaped and tilted T-shaped arrangements; also, the exchange-repulsion term is notably smaller. Effective induction energy is rather small, with the majority of the stabilization originating from effective dispersion energy, which, despite the larger distance in the stacked complex, is comparable for all three arrangements. The ratio E^{2*}_{disp}/E^1_{pol} is, however, significantly higher in the stacked arrangement than in both the T-shaped and tilted T-shaped ones (2.71 comparing to 1.45).

We have to conclude that similar interaction energies in the T-shaped and parallel arrangements arise from the complementarity of a repulsive E^1 term (the sum of E^1_{pol} and E^1_{ex}) and an attractive E^2 term (the sum of E^2_{ind}, E^2_{ex-ind}, E^2_{disp}, and $E^2_{ex-disp}$) energies. The E^1 term is more favorable (less repulsive) for the parallel arrangement, while the attractive E^2 energy is more favorable for the T-shaped arrangement.

Conclusions

The most stable arrangements found in optimizations of all three studied model systems are either T-shaped or tilted T-shaped; the energetic difference between these two arrangements is small, and no substantial barrier exists between these two minima. The interaction energies in both arrangements are large [up to −5.3 kcal/mol in NMA−benzene at the CCSD(T)/CBS level] and comparable to a classic H-bond. Such arrangements exist in proteins and, consequently, their contribu-

tion to protein stabilization should be quite significant. The size of the system brings a large increase of interaction, which is in accordance with the result of our previous work, where the calculated interaction energy in phenylalanine−NMF complex was −8.2 kcal/ mol.

The impressive performance of RI-DFT-D is notable. RI-DFT-D/LP stabilization energies agree well with the CCSD-(T)/CBS values, even though they require several orders of magnitude less CPU computational time. The MP2/aug-cc-pVDZ interaction energies are also very close to the CCSD-(T)/CBS ones, probably due to cancellation of errors. It is, however, not advisable to rely on this cancellation.

Decomposition analysis of interaction energy in T-shaped, tilted T-shaped, and parallel arrangements that exist in proteins was performed. All the arrangements exhibit comparable interaction energies in DFT-SAPT, which is an important observation in light of the fact that H-bonding (expected to be a dominant stabilization feature) exists only in the former two arrangements. The interaction energy decomposition indicated different natures of their stabilization due to the complementarity between repulsive E^1 and attractive E^2 energies. Dispersion energy is a major stabilizing term in stacked as well as T-shaped structures; however, they differ significantly in the $E^{2*}_{\mathrm{disp}}/E^{1}_{\mathrm{pol}}$ ratio.

Acknowledgment. This work was supported by Grants 203/05/0009 and 203/06/1727 from the Grant Agency of the Czech Republic and Grant LC512 from the Ministry of Education (MSMT) of the Czech Republic. It was also part of research projects Z40550506 and MSM6198959216. We are grateful to Kevin E. Riley for his comments and help with language corrections.

References and Notes

(1) Frank, B. S.; Vardar, D.; Buckley, D. A.; McKnight, C. J. The role of aromatic residues in the hydrophobic core of the villin headpiece subdomain. *Protein Sci.* **2002**, *11* (3), 680−687.

(2) Meyer, E. A.; Castellano, R. K.; Diederich, F. Interactions with aromatic rings in chemical and biological recognition. *Angew. Chem., Int. Ed.* **2003**, *42* (11), 1210−1250.

(3) Burley, S. K.; Petsko, G. A. Aromatic-Aromatic Interaction: a Mechanism of Protein Structure Stabilization. *Science* **1985**, *229* (4708), 23−28.

(4) Burley, S. K.; Petsko, G. A. Dimerization Energetics of Benzene and Aromatic Amino Acid Side Chains. *J. Am. Chem. Soc.* **1986**, *108* (25), 7995−8001.

(5) Chipot, C.; Jaffe, R.; Maigret, B.; Pearlman, D. A.; Kollman, P. A. Benzene dimer: A good model for π-π interactions in proteins? A comparison between the benzene and the toluene dimers in the gas phase and in an aqueous solution. *J. Am. Chem. Soc.* **1996**, *118* (45), 11217−11224.

(6) Hobza, P.; Selzle, H. L.; Schlag, E. W. Potential energy surface for the benzene dimer. Results of ab initio CCSD(T) calculations show two nearly isoenergetic structures: T-shaped and parallel-displaced. *J. Phys. Chem.* **1996**, *100* (48), 18790−18794.

(7) Muller-Dethlefs, K.; Hobza, P. Noncovalent interactions: A challenge for experiment and theory. *Chem. Rev.* **2000**, *100* (1), 143−167.

(8) Hobza, P.; Zahradnik, R.; Muller-Dethlefs, K. The world of non-covalent interactions: 2006. *Collect. Czech. Chem. Commun.* **2006**, *71* (4), 443−531.

(9) Zhao, Y.; Tishchenko, O.; Truhlar, D. G. How well can density functional methods describe hydrogen bonds to π acceptors? *J. Phys. Chem. B* **2005**, *109* (41), 19046−19051.

(10) Tsuzuki, S.; Honda, K.; Uchimaru, T.; Mikami, M.; Tanabe, K. Origin of the attraction and directionality of the NH/π interaction: Comparison with OH/π and CH/π interactions. *J. Am. Chem. Soc.* **2000**, *122* (46), 11450−11458.

(11) Steiner, T.; Koellner, G. Hydrogen bonds with π-acceptors in proteins: Frequencies and role in stabilizing local 3D structures. *J. Mol. Biol.* **2001**, *305* (3), 535−557.

(12) Mitchell, J. B. O.; Nandi, C. L.; Mcdonald, I. K.; Thornton, J. M.; Price, S. L. Amino/Aromatic Interactions in Proteins: Is the Evidence Stacked Against Hydrogen Bonding? *J. Mol. Biol.* **1994**, *239* (2), 315−331.

(13) Flocco, M. M.; Mowbray, S. L. Planar Stacking Interactions of Arginine and Aromatic Side-Chains in Proteins. *J. Mol. Biol.* **1994**, *235* (2), 709−717.

(14) Singh, J.; Thornton, J. M. Sirius: An Automated-Method for the Analysis of the Preferred Packing Arrangements Between Protein Groups. *J. Mol. Biol.* **1990**, *211* (3), 595−615.

(15) Nishio, M.; Hirota, M.; Umezawa, Y. The CH/pi Interaction; Wiley−VCH: New York, 1998.

(16) Toth, G.; Watts, C. R.; Murphy, R. F.; Lovas, S. Significance of aromatic−backbone amide interactions in protein structure. *Proteins: Struct., Funct., Genet.* **2001**, *43* (4), 373−381.

(17) Perutz, M. F. The Role of Aromatic Rings As Hydrogen-Bond Acceptors in Molecular Recognition. *Philos. Trans. R. Soc. London, Ser. A* **1993**, *345* (1674), 105−112.

(18) Duan, G. L.; Smith, V. H.; Weaver, D. F. An ab initio and data mining study on aromatic−amide interactions. *Chem. Phys. Lett.* **1999**, *310* (3−4), 323−332.

(19) Cheng, J. G.; Kang, C. M.; Zhu, W. L.; Luo, X. M.; Puah, C. M.; Chen, K. X.; Shen, J. H.; Jiang, H. L. *N*-Methylformamide-benzene complex as a prototypical peptide N-H$\cdots\pi$ hydrogen-bonded system: Density functional theory and MP2 studies. *J. Org. Chem.* **2003**, *68* (19), 7490−7495.

(20) Vondrasek, J.; Bendova, L.; Klusak, V.; Hobza, P. Unexpectedly strong energy stabilization inside the hydrophobic core of small protein rubredoxin mediated by aromatic residues: Correlated ab initio quantum chemical calculations. *J. Am. Chem. Soc.* **2005**, *127* (8), 2615−2619.

(21) Halkier, A.; Helgaker, T.; Jorgensen, P.; Klopper, W.; Koch, H.; Olsen, J.; Wilson, A. K. Basis-set convergence in correlated calculations on Ne, N-2, and H_2O. *Chem. Phys. Lett.* **1998**, *286* (3−4), 243−252.

(22) Jurecka, P.; Hobza, P. On the convergence of the ($\Delta E^{\mathrm{CCSD(T)}}-\Delta E^{\mathrm{MP2}}$) term for complexes with multiple H-bonds. *Chem. Phys. Lett.* **2002**, *365* (1−2), 89−94.

(23) Becke, A. D. Density-Functional Thermochemistry. 3. The Role of Exact Exchange. *J. Chem. Phys.* **1993**, *98* (7), 5648−5652.

(24) Zhao, Y.; Truhlar, D. G. Design of density functionals that are broadly accurate for thermochemistry, thermochemical kinetics, and nonbonded interactions. *J. Phys. Chem. A* **2005**, *109* (25), 5656−5667.

(25) Jurecka, P.; Cerny, J.; Hobza, P.; Salahub, D. R. Density functional theory augmented with an empirical dispersion term. Interaction energies and geometries of 80 noncovalent complexes compared with ab initio quantum mechanics calculations. *J. Comput. Chem.* **2007**, *28* (2), 555−569.

(26) Hesselmann, A.; Jansen, G.; Schutz, M. Density-functional theory−symmetry-adapted intermolecular perturbation theory with density fitting: A new efficient method to study intermolecular interaction energies. *J. Chem. Phys.* **2005**, *122* (1).

(27) Hesselmann, A.; Jansen, G.; Schutz, M. Interaction energy contributions of H-bonded and stacked structures of the AT and GC DNA base pairs from the combined density functional theory and intermolecular perturbation theory approach. *J. Am. Chem. Soc.* **2006**, *128* (36), 11730−11731.

(28) Frisch, M. J.; Trucks, G. W.; Schlegel, H. B.; Scuseria, G. E.; Robb, M. A.; Cheeseman, J. R.; Montgomery, J. A., Jr.; Vreven, T.; Kudin, K. N.; Burant, J. C.; Millam, J. M.; Iyengar, S. S.; Tomasi, J.; Barone, V.; Mennucci, B.; Cossi, M.; Scalmani, G.; Rega, N.; Petersson, G. A.; Nakatsuji, H.; Hada, M.; Ehara, M.; Toyota, K.; Fukuda, R.; Hasegawa, J.; Ishida, M.; Nakajima, T.; Honda, Y.; Kitao, O.; Nakai, H.; Klene, M.; Li, X.; Knox, J. E.; Hratchian, H. P.; Cross, J. B.; Bakken, V.; Adamo, C.; Jaramillo, J.; Gomperts, R.; Stratmann, R. E.; Yazyev, O.; Austin, A. J.; Cammi, R.; Pomelli, C.; Ochterski, J. W.; Ayala, P. Y.; Morokuma, K.; Voth, G. A.; Salvador, P.; Dannenberg, J. J.; Zakrzewski, V. G.; Dapprich, S.; Daniels, A. D.; Strain, M. C.; Farkas, O.; Malick, D. K.; Rabuck, A. D.; Raghavachari, K.; Foresman, J. B.; Ortiz, J. V.; Cui, Q.; Baboul, A. G.; Clifford, S.; Cioslowski, J.; Stefanov, B. B.; Liu, G.; Liashenko, A.; Piskorz, P.; Komaromi, I.; Martin, R. L.; Fox, D. J.; Keith, T.; Al-Laham, M. A.; Peng, C. Y.; Nanayakkara, A.; Challacombe, M.; Gill, P. M. W.; Johnson, B.; Chen, W.; Wong, M. W.; Gonzalez, C.; Pople, J. A. *Gaussian 03*, Revision C.02; Gaussian, Inc.: Wallingford, CT, 2004.

(29) Ahlrichs, R.; Bar, M.; Haser, M.; Horn, H.; Kolmel, C. Electronic-Structure Calculations on Workstation Computers the Program System Turbomole. *Chem. Phys. Lett.* **1989**, *162* (3), 165−169.

(30) Werner, H.-J.; Knowles, P. J.; Lindh, R.; Manby, F. R. Schütz, M.; Celani, P.; Korona, T.; Rauhut, G.; Amos, R. D.; Bernhardsson, A.; Berning, A.; Cooper, D. L.; Deegan, M. J. O.; Dobbyn, A. J.; Eckert, F.; Hampel, C.; and Hetzer, G.; Lloyd, A. W.; McNicholas, S. J.; Meyer, W.; Mura, M. E.; Nicklass, A.; Palmieri, P.; Pitzer, R.; Schumann, U.; Stoll, H.; Stone, A. J.; Tarroni, R.; Thorsteinsson, T. MOLPRO, version 2006.1: a package of ab initio programs.